



# Variations in the sediment phosphorus fractions and their release according to precipitation in the Han River, South Korea

Haeseong Oh<sup>1</sup> · Jung Hyun Choi<sup>1</sup>

Received: 25 July 2022 / Accepted: 6 February 2023 / Published online: 4 April 2023  
© The Author(s), under exclusive licence to Springer-Verlag GmbH Germany, part of Springer Nature 2023

## Abstract

**Purpose** In this study, we investigated the temporal and spatial variations of the inorganic phosphorus (P) fractions and their release using sediment collected from three weirs built along the Han River in South Korea.

**Methods** Sediment and water samples that were collected upstream of Gangcheon, Yeosu, Ipo weir in rainy and non-rainy seasons were incubated during 0, 3, and 7 days. The inorganic P fraction concentrations of the sediment sample were analyzed after incubation.

**Results** The sum of the four inorganic P fractions was significantly higher in the non-rainy season than in the rainy season. The P fractions with the highest concentrations, reductant soluble P- and Ca-bounded P, were also higher in the non-rainy season than in the rainy season. From the incubation experiment, it was observed that the concentration of inorganic P in the sediments tends to decrease with the incubation time in the non-rainy season resulting in the significant correlation between changes in Al- and Fe-bounded P in the sediment and PO<sub>4</sub>-P concentration in the overlying water layer. Sediments of three weirs were dominantly affected by non-point sources as indicated by EF (enrichment factor) value using P fractions. The Al-bounded P release rate was positively correlated with the pH, while those of the Fe- and Ca-bounded P were correlated with the organic matter.

**Conclusion** The fractionation and release of P in the sediments was affected by the rainfall and physiochemical factors. The results of this study will enhance our understanding of the water quality, as well as the effects of impoundment and rainfall on sediment, thereby aiding in an efficient management of the river environment.

**Keywords** Inorganic phosphorus fractions · Rainfall pattern · Phosphorus release · Sediments · Han River

## 1 Introduction

The element phosphorus (P), which has been recognized as an important nutrient for primary productivity, is a limiting element in the rivers (Kaiserli et al. 2002; Bao et al. 2020; Jin et al. 2020). An excessive loading and accumulation of P on the river sediments can lead to the degradation of water quality and cause frequent eutrophication—a fate shared by many rivers around the world (Santos et al. 2015;

Huang et al. 2018). The impoundment by hydraulic structures increases sediment deposition in the river bed, and these P-rich sediments release a significant concentration of P into the water column, thereby degrading the water quality (eutrophication of impounded water; Chen et al. 2017; Renwick et al. 2005; Table S1). Incidentally, all hydraulic structures, ranging from large well-established dams to small weirs, can efficiently retain P-rich sediments (Nemery et al. 2016; Bao et al. 2020).

External point sources such as domestic and industrial wastewater, and non-point sources such as runoff and soil leaching due to rainfall are the main source of P in rivers. Sediment P concentration and its fractional composition can be differentiated by P pollution sources. The P fractions in river sediments are divided into several categories such as labile P, the fraction associated with oxides and hydroxides of Al, Fe, Mg, and Mn (non-apatite P), calcium-associated

Responsible editor: Shiming Ding

✉ Jung Hyun Choi  
jchoi@ewha.ac.kr

<sup>1</sup> Department of Environmental Science and Engineering, Ewha Womans University, 52, Ewhayeodae-Gil, Seodaemun-Gu, Seoul 03760, Korea

P, reductant soluble P (Red-P), and organic P (Wang et al. 2005; Bao et al. 2020). Sediments impacted by point sources have a higher proportion of P associated with Al and Fe, while those impacted by non-point sources have a higher proportion of P associated with Ca. The P fractional composition could indicate P pollution sources to distinguish the relative contribution of point and non-point sources which support P control strategies of the watershed.

Rainfall introduces various combinations of P loadings, which transfer from the sediment to the water column via various physical and biochemical reactions such as precipitation, ion exchange, and adsorption (Kim et al. 2003; Sun et al. 2009). Moreover, when the quality of the overlying water changes, P can be released from the sediment to the water column via diverse mechanisms such as molecular diffusion, advection, and biologically mediated changes (Furumai et al. 1989; Kim et al. 2003). In addition, the release of P from the sediment depends on the P fractions, water flow, and physiochemical properties of the sediment and water column. Among these P fractions, the P associated with Al and Fe can affect the P sorption on sediment surfaces (Borggaard et al. 1990). Under a low concentration of dissolved oxygen in a water column, the P solubility is mostly related to the P associated with Fe (Olia and Redy 1997). Non-apatite P as well as organic P can be easily released or mineralized into water and maintain the eutrophic state for a long duration. Non-apatite P is well absorbed by plants, and it can be easily released into the water layer by responding to environmental changes (Ki et al. 2010; Kim et al. 2005). Therefore, it is necessary to evaluate sediment P concentration and P-fractions which determine the effect of sediment on water quality by estimating P contamination levels, bioavailability, and potential mobility under different environmental factors.

Furthermore, the P release can vary depending on the physiochemical factors of the sediment and water column, such as the dissolved oxygen concentration, pH, temperature, concentration of nutrients, and flow conditions (Li et al. 2013; Vilmin et al. 2015; Orihel et al. 2017). According to the previous studies, a larger amount of P is released under alkaline, high-temperature, anaerobic, and high-nutrient-concentration conditions (Jensen and Andersen 1992; Li et al. 2013; Wu et al. 2014; Ma et al. 2018). However, because the release of P from the sediments to the water column results from a combination of various mechanisms, it is difficult to identify the physiochemical factors that predominantly contribute to this process (Kaiserli et al. 2002).

In several studies, the potential P release was found to be higher from the sediments retained by the hydraulic structure (Kim et al. 2003; Oh et al. 2017). However, the role of rainfall-induced P-loading and P-fraction release rates have been rarely investigated. Along the Han River in South Korea, three consecutive weirs are present, which affect the accumulation of P on the sediment. The P loading induced

by rainfall modulate the fraction and physiochemical factors, which may affect the P release and cause long-term eutrophication of the impoundments. To date, several studies based on the physical and chemical properties of the sediments such as particle size, organic matter, and nutrient content in the weirs of Han River have been reported (Vo et al. 2014). However, only a few investigations have been conducted to assess the effect of rainfall on the P fraction and its release. Therefore, this study was undertaken to (1) investigate the temporal variations of inorganic P fractions in the sediments of Han River; (2) estimate their release to the overlying water, via incubation experiments; and (3) analyze the physiochemical factors that determine the transport of inorganic P in the sediments. The results obtained in this study will improve the understanding of the effects of impoundment and rainfall characteristics on the sediment and water quality—crucial for an efficient management of the river environment.

## 2 Methods

### 2.1 Site description

This study was conducted within the Han River watershed, which is 375 km long, covers an area of 23,859 km<sup>2</sup> along the primary river (Park et al. 2008; Lee et al. 2012), and is located in the eastern region of South Korea. There are three weirs in the Namhan River (Gangcheon, Yeosu, and Ipo Weir). The length and height of Gangcheon weir are 440 m and 8 m. The length and height of Yeosu weir are 513 m and 8 m. The length and height of Ipo weir are 521 m and 6 m (Korea Water Resources Corporation; Oh and Choi 2022; Table S2). In 2016 and 2017, the annual average temperatures of this watershed were 13.0 °C (−13.5–30.0 °C) and 12.3 °C (−9.8–29.9 °C), respectively. Additionally, its hydrologic characteristics are affected by the East Asian summer monsoon climate, such that over 50% of the recorded annual precipitation is observed from late June to early September. In the Gangcheon, Yeosu, and Ipo weirs of the Han River, the annual precipitation from 2013 to 2017 was 810.8 to 1314.6 mm, and the precipitation of summer monsoon was 384.9 to 964.4 mm (Table S3). The amount of summer monsoon precipitation ranged from 46 to 84% of the annual precipitation (K-water, <http://www.water.or.kr>, 2013–2017). From the ratio of summer monsoon and annual precipitation, it can be seen that most precipitation was concentrated in summer.

### 2.2 Sampling and pretreatment

As a part of a large river restoration project designed to control flooding and water supply, multipurpose weirs have

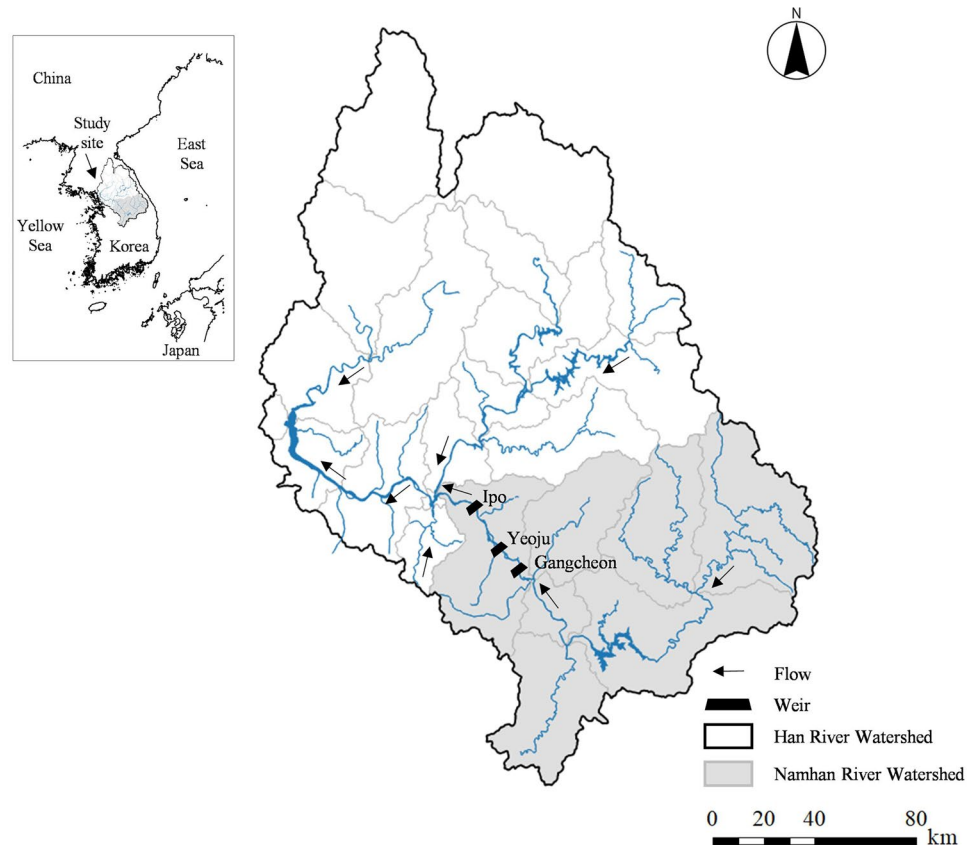
been constructed along the Han River (Fig. 1). Weir construction facilitates the accumulation of sediments near the weirs and thus significantly impacts the quantity and quality of P concentrations in these accumulated sediments (Bao et al. 2020). In addition, water quality issues such as DO depletion in the bottom water and algal bloom can be occurred in the 1 km upstream of the weirs. Therefore, the temporal and spatial variation of the P fractions and their release were investigated to analyze the effect of sediments on the water quality in the 1 km upstream of the weirs. During 2016–2017, sediment samples were collected upstream of the Gangcheon ( $37^{\circ}16'29.50''\text{N}$ ,  $127^{\circ}41'13.70''\text{E}$ ), Yeosu ( $37^{\circ}19'9.10''\text{N}$ ,  $127^{\circ}37'14.80''\text{E}$ ), and Ipo weir ( $37^{\circ}24'8.30''\text{N}$ ,  $127^{\circ}32'29.00''\text{E}$ ) four times (August and October 2016, May and June 2017). Because rainfall affects the P concentration in the sediment (Vo et al. 2014), the sampling was divided into two periods: rainy and non-rainy seasons. Based on the rainfall pattern in the Han River watershed, the samples collected in August and October 2016 were classified as the rainy season samples, whereas those collected in May and June 2017 were classified as the non-rainy season samples. The rainy season samples were collected immediately after the heavy rainfall, whereas the non-rainy season samples were acquired when there was no rainfall for a long time, and the sediments were stabilized.

Incubation experiments were conducted on every sampling event of three weirs. For incubation, acrylic core samplers with top and bottom covers (diameter and height of 10 and 22 cm, respectively) were used by a scuba diver to collect a 15-cm high sediment core together with the overlying water. Three sediment cores were sampled for the incubation ( $n = 1$ ), as well as for the analysis of the sediment ( $n = 1$ ) and pore-water ( $n = 1$ ) chemistry at each weir. The bottom water was separately collected in separate bottles using a Niskin water sampler. The core tube and bottom water samples were carefully placed in an upright position without disturbance inside a closed ice box and transported to the laboratory (Lee et al. 2018).

The sediment samples were retrieved from the upper part (0–2 cm) of the core and homogeneously mixed in a  $\text{N}_2$ -purged vinyl bag (Cho et al. 2002). Homogeneously mixed sediment (45 g) was placed in a 100-ml serum vial containing 70 mL of bottom water filtered using Whatman GF/F filters ( $0.7 \mu\text{m}$ , Thurman 2012). The top of each vial was sealed with glass wool to prevent evaporation of the overlying water. Then, these vials containing the sediment and bottom water samples were incubated to estimate the change in the P concentration in the sediments.

The laboratory incubation was carried out in a dark chamber at a constant ambient temperature of  $20 \text{ }^{\circ}\text{C}$  for up to

**Fig. 1** Map of the sampling location in the Han River basin, South Korea, showing the details of the sampling sites (Gangcheon, Yeosu, and Ipo weir)



7 days (Kalbitz et al. 2003; Luek et al. 2017). A total of nine vials were incubated for each site (Gangcheon, Yeosu, and Ipo weir). At 0, 3, and 7 days of incubation, three vials for each site were sacrificed for analysis (triplicate analysis), i.e., the sediment was collected without the supernatant, and the P fraction was measured three times.

### 2.3 Phosphorus fractions

Depending on the bond formation with metals or organic matter, the sediment P can be divided into various forms such as labile P, inorganic P, metal-bounded P, and organic P. Among these forms, the inorganic P is further divided into soluble, Al-bounded phosphate (Al-P), Fe-bounded phosphate (Fe-P), Red-P, and Ca-bounded phosphate (Ca-P). P can be efficiently released through inorganic phosphate by fraction rather than total P content in sediment of freshwater. The phosphate fractions were measured using the method proposed by Petersen and Corey (1966), in which the formation of inorganic phosphate via bonding with metals is analyzed for each metal, and the corresponding procedures are as follows (Fig. S1; Wang et al. 2005; Aydin et al. 2010; Yang et al. 2020):

**Remove the loosely bound P:** Place approximately 1 g of the sediment sample in the centrifuge tube. Next, add 50 mL of 1 N  $\text{NH}_4\text{Cl}$  and shake for 30 min to remove the soluble and loosely bound P. Finally, discard the supernatant solution and save the sediment in the tube for extraction of Al phosphate.

**Al-P ( $n = 108$ ):** Add 50 mL of 0.5 N  $\text{NH}_4\text{F}$  (pH 8.2) to the sediment sample and stir for 1 h. Next, add 3 mL of chloromolybdic boric acid solution and one drop of the chlorostannous reductant to 3 mL of the supernatant, and measure the absorbance at a wavelength of 660 nm.

**Fe-P ( $n = 108$ ):** After the Al-P measurement, wash the remaining sediment sample with saturated NaCl. Add 50 mL of NaOH to the washed sample, stir for 17 h, and subsequently add  $\text{H}_2\text{SO}_4$  to 50 mL of the supernatant. Next, add 3 mL of chloromolybdic boric acid solution and one drop of the chlorostannous reductant to 3 mL of the supernatant, and measure the absorbance at a wavelength of 660 nm.

**Red-P ( $n = 108$ ):** After the Fe-P measurement, wash the remaining sample with saturated NaCl, and then add 25 mL of 0.3 M  $\text{Na}_3\text{C}_6\text{H}_5\text{O}_7 \cdot 2\text{H}_2\text{O}$  and 1 g of  $\text{Na}_2\text{S}_2\text{O}_4$  (solid) to it and heat in a water bath at 75–80 °C. Add 1.5 mL of 0.25 M  $\text{KMnO}_4$ , 3 mL of an ammonium molybdate-sulfuric acid reagent, and 10 mL of isobutyl alcohol to 3 mL of the supernatant, and shake until the alcohol layer is mixed. When the alcohol layer is separated, separate 5 mL of liquid from the alcohol layer and add 3 mL of a stannous chloride reductant to it. Finally, separate 3 mL of this resulting solution, add 3 mL of absolute ethyl alcohol to it, and measure the absorbance at 660 nm.

**Ca-P ( $n = 108$ ):** Wash the soil sample used for Red-P fraction measurement. Add 50 mL of 0.5 N  $\text{H}_2\text{SO}_4$  to this washed

sample and stir for an hour. Next, add 3 mL of chloromolybdic boric acid solution and one drop of the chlorostannous reductant to 3 mL of the supernatant, and measure the absorbance at a wavelength of 660 nm.

The P-fraction release rate ( $\text{g m}^{-2} \text{day}^{-1}$ ) was calculated that the difference of each P fraction concentration between 0 and 3 days was multiplied by the volume of the supernatant in the sample vial which was divided by the surface area of sediment and the number of incubation days.

The ratio of Al + Fe-P and Ca-P is used to differentiate the relative contribution of point sources and nonpoint sources (Liu et al. 2012). Many studies have reported that the urbanized area affected by point sources showed higher concentration of P with dominant Al-P and Fe-P, while the agricultural area affected by nonpoint sources showed the lowest concentration of P with dominant Ca-P (Liu et al. 2012; Yang et al. 2020; Zhang et al. 2022). The enrichment factor (EF) is calculated by  $(\text{Al} + \text{Fe-P}/\text{Ca-P})$  of the surface sediment dividing by  $(\text{Al} + \text{Fe-P}/\text{Ca-P})$  of the background sediment ( $n = 108$ ). The EF value of  $\leq 1$  indicates a greater contribution of nonpoint sources, and the EF value of  $> 1$  indicates a greater contribution of point sources in sediment P (Zhang et al. 2022). The  $(\text{Al} + \text{Fe-P}/\text{Ca-P})$  of the background sediment was set to be 1.753, achieved from the average ratio of Fe + Al-P/Ca-P of the previous study in Namhan River (Jun 1990). Since Jun (1990) had measured the P fraction in the sediment of the Namhan River at least 30 years ago, the value was used as the value of background sediment in this study.

### 2.4 Analytical methods

The in situ temperature, pH, and DO concentration of the surface and bottom water layers were measured using a multiparameter instrument (professional plus, YSI, USA). The physical and chemical characteristics of the sediments, including the  $\text{NO}_2\text{-N}$ ,  $\text{NO}_3\text{-N}$ , and dissolved organic carbon (DOC) of the overlying water, as well as the surface sediment particle size, total organic carbon (TOC) and chlorophyll-a content, and  $\text{PO}_4\text{-P}$  release rate, were evaluated.

The concentrations of  $\text{NO}_2\text{-N}$  and  $\text{NO}_3\text{-N}$  were measured using ion chromatography (790 Personal IC, Metrohm, Switzerland). The DOC concentrations were measured using a TOC analyzer (V-CPH, Shimadzu, Japan). After removing the particulate organic carbon using a GF/F filter, the DOC was measured using a non-purgeable organic carbon method.

The particle size was determined by sieving the sediments and using an automatic particle size analyzer after removing the carbonate and organic matter using hydrogen peroxide (Mastersizer 2000, Malvern, UK). The sediment samples were freeze-dried and crushed in an agate mortar. Then, an elemental analyzer (EA 1110, GV instruments, UK) was used to determine the TOC after removing the inorganic carbonate using 1.0 N HCl acid. To measure the chlorophyll-a

content, the surface sediment samples (2 mL) were extracted in 10 mL of 90% v/v acetone for 24 h in a dark refrigerator, and then centrifuged before decanting into a cuvette. This cuvette was then analyzed using a UV-2401 PC (Shimadzu).

To estimate PO<sub>4</sub>-P release rate, the overlying water samples were collected every 1 or 1 h up to 10 h during the incubation and the changes of the PO<sub>4</sub>-P concentration were analyzed using ion chromatography (790 Personal IC, Metrohm, Switzerland). The PO<sub>4</sub>-P release rate was calculated by multiplying the slope of PO<sub>4</sub>-P concentration changes and volume of the supernatant divided by the sediment surface area.

## 2.5 Statistical methods

Statistical analyses were performed to identify the factors that significantly correlate with the characteristics of P-fraction ( $p < 0.05$ ). A linear regression analysis of the relationship between the P fraction characteristics and the physiochemical factors was performed (Sigmaplot 10.0, Systat Software, USA). Further, principle component analysis (PCA) was conducted to correlate the P fraction and the physiochemical factors, using Unscrambler X 10.1 (CAMO software, Norway). PCA is a multivariate discrimination method that reduces the dimension of a group of data and enables transformation with a reduced number of variables to distribute the data intuitively (Anzano et al. 2011).

## 3 Results and discussion

### 3.1 Physical and chemical characteristics of the Han River

The water depth, sediment particle size, temperature, pH, and DO concentration of the surface and bottom water layers were measured at the sampling sites, and the corresponding

results are shown in Table 1. The water depth ranged from 1.0 to 5.7 m over the entire sampling period, with the shallowest water depth recorded at the Ipo weir in June 2017, whereas the deepest depth was recorded at the Gangcheon weir in June 2017.

The average surface and bottom water temperatures were  $24.4 \pm 2.17$  and  $25.1 \pm 2.85$  °C in the rainy season (August and October 2016) and  $20.61 \pm 2.88$  and  $20.21 \pm 2.86$  °C in the non-rainy season (Table 1). The temperatures of the surface and bottom water layers were significantly higher in the rainy season (August 2016) than in the non-rainy season (May 2017; one-way ANOVA,  $p < 0.05$ ;  $n = 12$ ). Additionally, the differences between the surface and the bottom water temperatures were below 2 °C across all the sampling sites and over the entire sampling period, and no stratification was observed.

The DO concentrations of the surface and bottom water layers were  $8.91 \pm 1.20$  and  $8.52 \pm 1.56$  mg L<sup>-1</sup>, respectively. Because the degree of DO saturation of the bottom water layer was in the range of 71–135%, no oxygen depletion was observed. The pH of the bottom water layer was  $7.74 \pm 0.44$ . Evidently, the pH in the non-rainy season (May and Jun 2017) was higher than that in the rainy season (August and October 2016;  $t$  test,  $p = 0.043$ ;  $n = 12$ ). However, no significant difference between the pH of the sampling sites was observed (one-way ANOVA,  $p > 0.05$ ).

The NO<sub>x</sub> (NO<sub>2</sub> + NO<sub>3</sub>) concentration and DOC of the overlying water were in the range of 0.81–2.08 and 0.37–3.48 mg L<sup>-1</sup>, respectively. The NO<sub>x</sub> and DOC concentration of the overlying water was higher in the rainy season (August and October 2016) than in the non-rainy season (May and June 2017;  $t$  test,  $p < 0.05$ ;  $n = 12$ ). However, no significant difference between sampling sites was observed ( $n = 12$ ).

The sediment particle size ranged from 0.013 to 0.363 mm at the Gangcheon weir, from 0.029 to 0.068 nm

**Table 1** Physical and chemical characteristics of the Han River

		Water depth (m)	Particle size (mm)	Surface temp (°C)	Bottom temp. (°C)	Surface DO (mg L <sup>-1</sup> )	Bottom DO (mg L <sup>-1</sup> )	Precipitation (average of 28 days; mm day <sup>-1</sup> )
Gang cheon	Range	2.6–5.7	0.013–0.363	15.9–23.5	15.5–22.0	7.6–10.1	6.3–9.9	0.72–7.76
	Average	$3.6 \pm 1.5$	$0.135 \pm 0.197$	$20.6 \pm 3.3$	$20.1 \pm 3.1$	$8.9 \pm 1.3$	$8.2 \pm 1.5$	$3.11 \pm 3.27$
Yeouju	Range	1.7–2.2	0.029–0.068	19.3–25.7	18.5–27.6	7.7–9.8	6.8–10.2	0.42–3.73
	Average	$2.0 \pm 0.2$	$0.042 \pm 0.022$	$22.8 \pm 2.9$	$22.9 \pm 3.9$	$8.7 \pm 0.9$	$8.5 \pm 1.6$	$1.89 \pm 1.37$
Ipo	Range	1.0–3.5	0.056–0.230	18.2–25.6	18.1–25.7	7.5–11.4	7.5–11.5	0.86–10.08
	Average	$2.3 \pm 1.0$	$0.118 \pm 0.097$	$21.3 \pm 3.7$	$21.3 \pm 3.8$	$9.2 \pm 1.7$	$9.0 \pm 1.9$	$3.8 \pm 4.32$
Rainy season	Range	1.7–3.5	0.030–0.230	18.2–25.7	18.1–27.6	7.5–8.9	6.8–9.5	1.8–10.08
	Average	$2.5 \pm 0.6$	$0.097 \pm 0.115$	$22.4 \pm 2.9$	$22.6 \pm 3.4$	$8.1 \pm 0.5$	$8.0 \pm 0.9$	$4.94 \pm 3.23$
Non-rainy season	Range	1.0–5.7	0.013–0.363	15.9–24.4	15.5–24.4	7.7–11.4	6.3–11.5	0.42–1.59
	Average	$2.7 \pm 1.7$	$0.100 \pm 0.131$	$20.8 \pm 3.4$	$20.3 \pm 3.4$	$9.7 \pm 1.2$	$9.1 \pm 1.9$	$0.93 \pm 0.39$



at the Yeosu weir, and from 0.056 to 0.23 mm at the Ipo weir. The sediment distribution triangle contained silt loam (October 2016, May 2017 at Gangcheon and Yeosu), sandy loam (June 2017 at Gangcheon and Yeosu, and May and June 2017 at Ipo), sand (October 2016 at Ipo; Fig. 2). The particle sizes, observed during the different sampling periods at the different sampling sites, did not show any significant difference ( $n = 12$ ). The TOC and chlorophyll-a concentrations of the surface sediment were in the range of 0.36–3.59% and 7.78–69.13  $\mu\text{g cm}^{-3}$ , respectively, and showed no difference during the sampling periods at the different sampling sites.

The residence time was  $0.58 \pm 0.30$  days in the rainy season, and  $1.91 \pm 0.40$  days in the non-rainy season. Furthermore, the precipitation was  $7.19 \pm 3.21$  mm  $\text{days}^{-1}$  in the rainy season, and  $1.52 \pm 1.01$  mm  $\text{days}^{-1}$  in the non-rainy season (Fig. 3). Evidently, significant differences were observed between the residence times and precipitations during the different sampling periods as well as during the rainy and non-rainy seasons (one-way ANOVA,  $p < 0.05$ ;  $n = 12$ ).

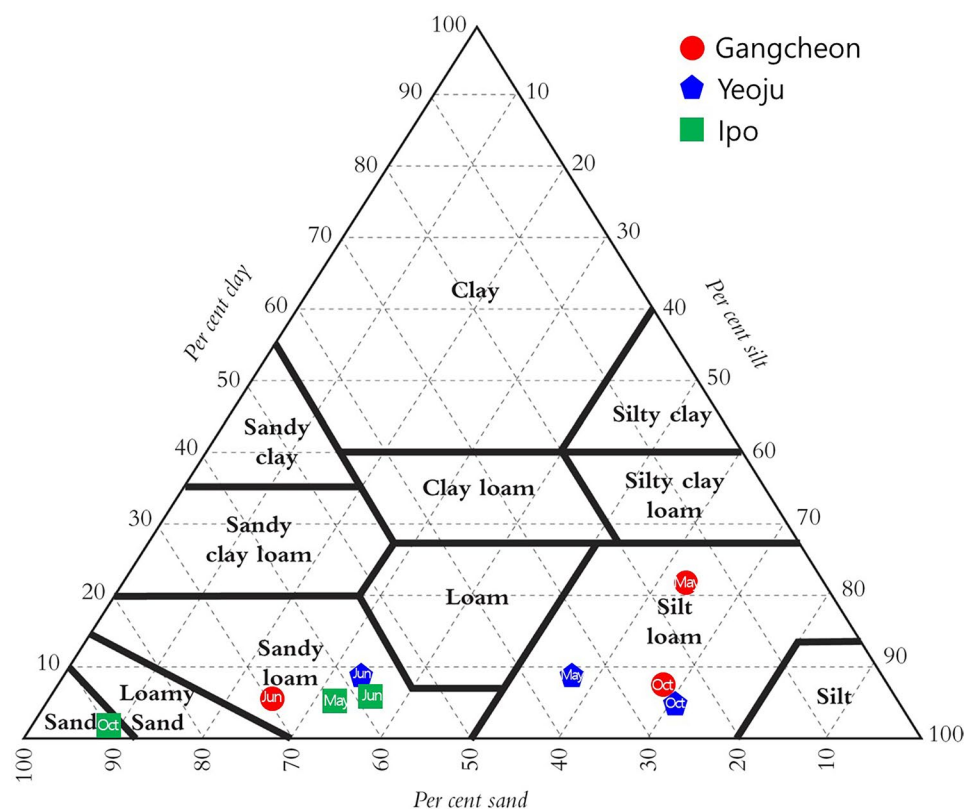
### 3.2 Phosphorus fraction in the sediments

Figure 4 shows the different P fractions (Fig. 4a) and their relative contributions (Fig. 4b) according to the sampling locations and periods, indicating that the sum of the four inorganic P fractions (Al-P, Fe-P, Red-P, and Ca-P) ranges from 197.88 to 505.89  $\text{mg kg}^{-1}$ . This sum is significantly higher

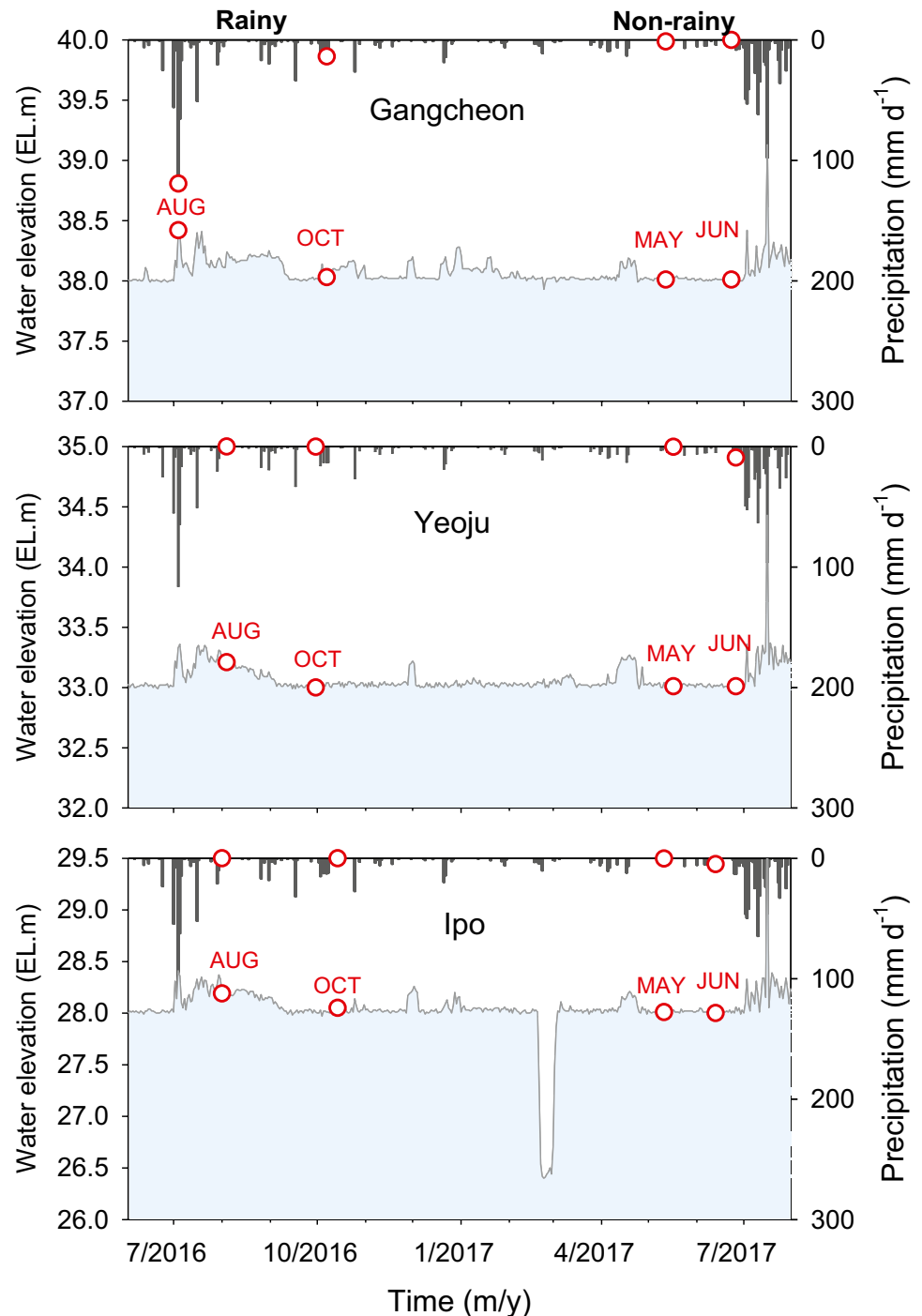
in the non-rainy season (May 2017, 427.68–458.04  $\text{mg kg}^{-1}$ ; June 2017, 437.43–505.89  $\text{mg kg}^{-1}$ ) than in the rainy season (August 2016, 197.88–232.51  $\text{mg kg}^{-1}$ ; October 2016, 211.03–267.16  $\text{mg kg}^{-1}$ ; one-way ANOVA,  $p < 0.05$ ;  $n = 36$ ). Reportedly, the concentration of P released from the sediments increases with the increasing flow rates due to rainfall (Yao et al. 2016; Jin et al. 2020). Therefore, it is estimated that the inorganic P concentration of the sediment was low in the rainy season (August and October 2016) with high flow rate, whereas it was relatively high in the non-rainy season (May and June 2017) with low flow rate. However, no difference between the P concentrations of the sampling sites at the Gangcheon, Yeosu, and Ipo weirs were observed (one-way ANOVA,  $p > 0.05$ ;  $n = 36$ ).

For the sediment samples, the P fractions were in the following order: Red-P > Ca-P > Al-P > Fe-P (one-way ANOVA,  $p < 0.05$ ;  $n = 36$ , respectively), similar to the distribution pattern reported by Kaiserli et al. (2002). Sediment P concentration and its fractions are important parameters that indicated P pollution level and potential availability under different environmental conditions. The concentrations of Al-P and Fe-P fractions ranged from 21.28 to 79.32  $\text{mg kg}^{-1}$  and from 4.29 to 32.02  $\text{mg kg}^{-1}$ , respectively, lower than those of the Red-P and Ca-P. The Al-P and Fe-P fractions were used to estimate available P in the sediments which results in P release and diffusion towards the water column through pore water under anoxic condition in subsurface

**Fig. 2** Particle size distribution of the Han River sediment



**Fig. 3** Water elevation and precipitation during the sampling period at the Gangcheon, Yeosu, and Ipo weirs. The circles indicate the date of collection of the sample in the upstream of the weirs



sediments (Zhou et al. 2001). Because the P content can be determined from the sediment properties, our analysis showed that the concentrations of Al-P and Fe-P were higher in the acidic sediment and lower in the others (Verma et al. 2005). There was no difference between Al-P and Fe-P according to the rainfall period (one-way ANOVA,  $p > 0.05$ ;  $n = 36$ ). Reportedly, the Al-P and Fe-P fractions can vary widely when anoxic conditions prevail at the overlying water of the sediment (Sun et al. 2009). Since oxic conditions were

maintained during the sampling period, it is estimated that the loading and release of Al-P and Fe-P remained constant, implying that there was no difference in the concentrations of Al-P and Fe-P.

The Red-P concentration was in the range of 115.20–325.51 mg kg<sup>-1</sup>, showing the highest concentration among all the four inorganic P fractions as well as indicating that this P fraction is sensitive to oxidation and is mainly composed of Fe-hydroxide and Mn-compound bounded P

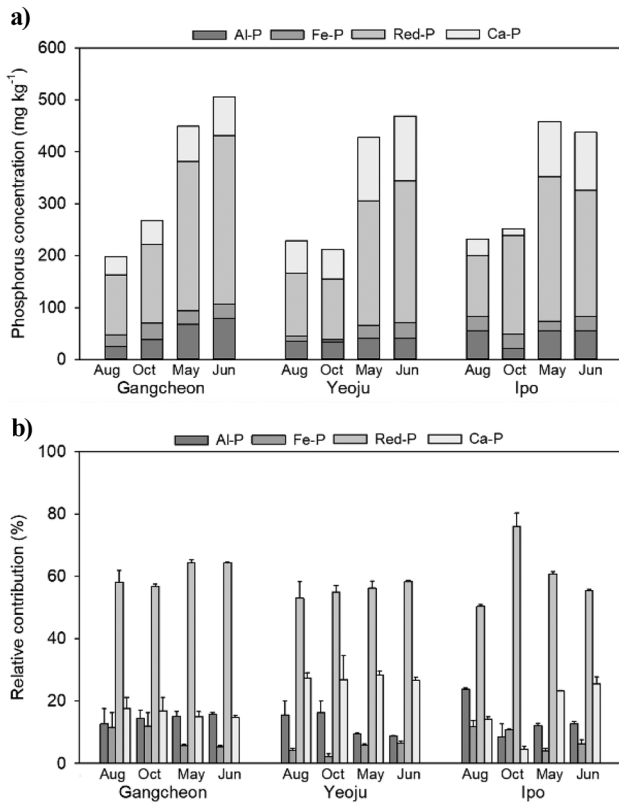


**Fig. 4** **a** Concentrations of different P fractions and **b** relative contribution of the P fractions according to sampling location and period

(Kozerski and Kleeberg 1998). The high Red-P concentrations both in the rainy and non-rainy seasons can be attributed to the oxic sediment surface that acts as boundary layer for the upward diffusing P such as the Fe- and Mn-bounded P (Kaiserli et al. 2002). The Red-P concentrations in the three weirs were higher in the non-rainy season (May and June 2017) than in the rainy season (August and October 2016; one-way ANOVA,  $p < 0.05$ ;  $n = 36$ ), same as the result of the sum of the four P fractions. This difference between the Red-P concentrations in the rainy and non-rainy seasons might be related to the trophic status at the sampling season. The lower organic content, especially DOC in sediment–water interface, in the non-rainy season acts as a favorable boundary layer for upward diffusing P, Fe, and Mn. However, there was no significantly difference between the Red-P concentrations of the three weirs.

The Ca-P fraction, which is mainly composed of apatite P, exhibited a large variability in the sediments of the three weirs. The concentration of Ca-P was in the range of 11.71–124.46 mg kg<sup>-1</sup>, which was the second highest value (after the Red-P concentration) among those of the four P-fractions. According to the previously reported studies, Ca-P exhibits the highest abundance among all the inorganic P fractions present in surface sediments (Aydin et al. 2010;

Thin et al. 2020), leading to the oversaturation of calcite, co-precipitation of phosphate, and mineralogical composition of the particles (Thin et al. 2020; Aydin et al. 2010). Based on the sampling period, the concentrations of Ca-P were higher in the non-rainy season (May and Jun 2017) than in the rainy season (August and October 2016; one-way ANOVA,  $p < 0.05$ ;  $n = 36$ ), similar to the concentrations of Red-P. No significant difference between the Ca-P concentrations at the three weirs was observed.

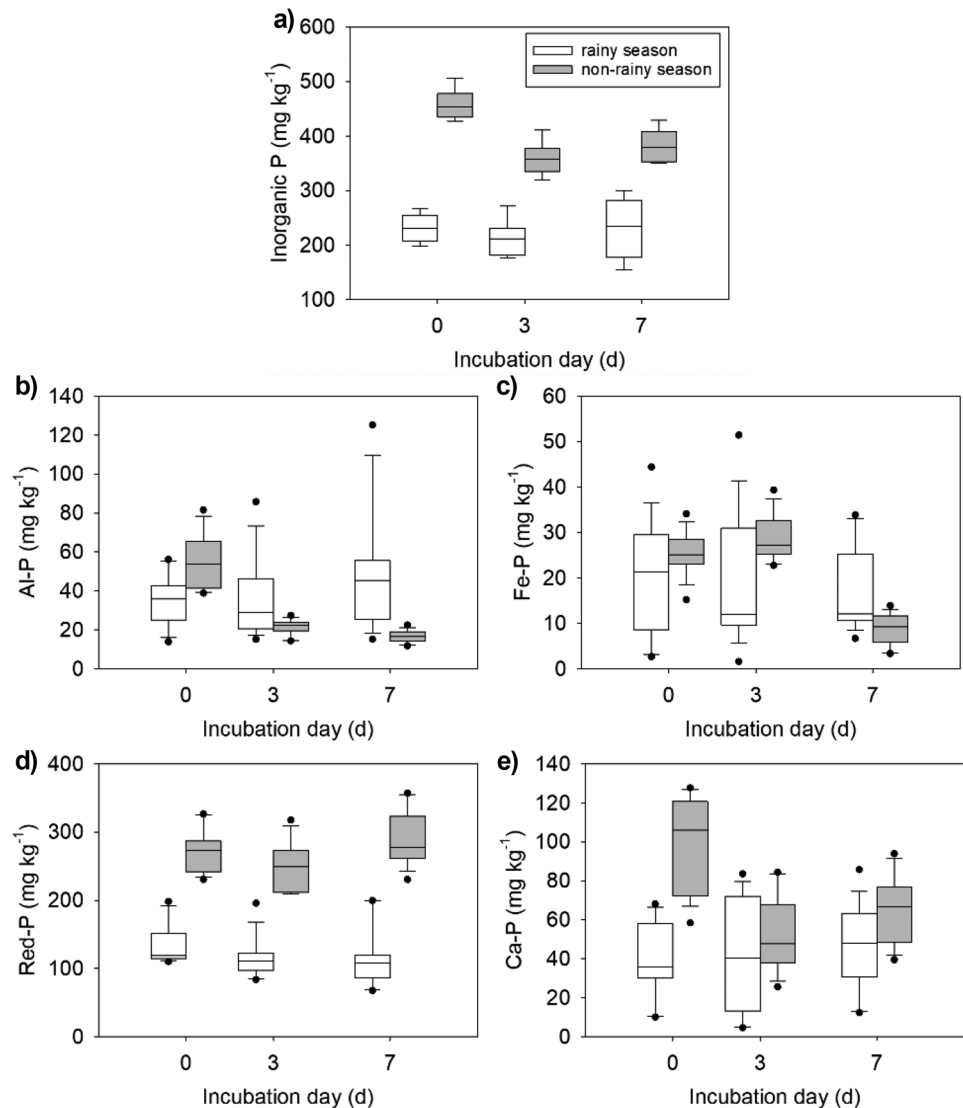
### 3.3 Variations in the sediment phosphorus release rates

The concentration of inorganic P during the incubation periods in the rainy (August and October 2016) and non-rainy seasons (May and June 2017) are depicted in Fig. 5. The concentration of inorganic P in the sediments did not change with the incubation time in the rainy season (August and October 2016; one-way ANOVA,  $p > 0.05$ ). However, it tended to decrease with the increasing incubation time in the non-rainy season (May and June 2017; one-way ANOVA,  $p < 0.05$ ; Fig. 5a). In the non-rainy season (May and June 2017), the sum of the concentrations of the four fractions decreased by 8–28% for three days (one-way ANOVA,  $p < 0.05$ ;  $n = 36$ ); afterwards, it was maintained or increased. Because the concentration of inorganic P in the sediment decreased with the incubation time, it was assumed that P was released from the sediment into the overlying water, similar to the results of the previous studies (Sun et al. 2009).

Reportedly, the change in the sediment P content is related to the composition of each P fraction (Nurnberg 1988; Jalali 2010). Therefore, the results of P concentration for each P fraction were examined, and the corresponding results are shown in Fig. 5b–e. In the rainy season (August and October 2016), there was no change in the concentrations of the four P fractions according to the incubation time. However, in the non-rainy season (May and June 2017), the Al-P, Fe-P, and Ca-P contents of the sediment decreased during the incubation time (one-way ANOVA,  $p < 0.05$ ;  $n = 36$ ). A concentration decreases of 45–71%, with a release rate of 0.34–1.04 g m<sup>-2</sup> day<sup>-1</sup>, was observed for the Al-P fraction during the 3-day incubation period. In contrast, although the release rate of Fe-P also decreased with the incubation time, but there was no change until 3 days. After 3 days, the Fe-P content of the sediment decreased by 59–89%, and the release rate was 0.24–0.38 g m<sup>-1</sup> day<sup>-1</sup>. For Ca-P, the concentration decrease was 31–62% with a release rate of 0.50–1.43 g m<sup>-2</sup> day<sup>-1</sup> during 3-day incubation period. This release rate was relatively smaller than those of Al-P and Fe-P. The opposite trend occurred for Red-P, which showed increasing concentration and release rate after 3 days of incubation. However, no statistically significant difference was identified (one-way ANOVA,  $p > 0.05$ ;  $n = 36$ ).



**Fig. 5** Changes in the inorganic P concentration during the incubation (7 days) of the samples obtained during the rainy season (August and October 2016) and non-rainy season (May and June 2017): **a** sum of the concentrations of all the four fractions, **b** Al-P concentration, **c** Fe-P concentration, **d** Red-P concentration, and **e** Ca-P concentration



Al-P and Fe-P are classified as non-apatite inorganic P (NAI-P; Nurnberg 1988). Al and Fe oxides combined with P in the sediments contain a number of minerals such as hematite, magnetite, amorphous Al oxides, and corundum (Wu et al. 2020). Among Al and Fe oxides, amorphous or amorphous form can be bind to P through co-precipitation of surface (Khare et al. 2005; Zhang et al. 2022). Even though NAI-P show different P adsorption or desorption capacity depending on the structure with minerals (Wu et al. 2020), NAI-P could indicate presence of mobile and bio-available P and used for the estimation of available P in the sediment (Zhou et al. 2001; Hou et al. 2014; Saha et al. 2022). Reportedly, the binding capacity of NAI-P is correlated with the pH of the water body (Jensen and Andersen 1992). Because the binding force of Al-P and Fe-P decreases with the increasing pH, a higher pH of the water implies a weaker bounding between P and the metals Fe and Al in the sediment, resulting in easy release of these inorganic P fractions into

the water layer. In this study, because the pH was higher in the non-rainy season (7.76–8.25; May and June 2017) than in the rainy season (6.91–7.61; August and October 2016), the decrease in the concentrations of Al-P and Fe-P was more distinguishable in the non-rainy season than in the rainy season.

Further, the correlation between the Al-P and Fe-P release rates and the PO<sub>4</sub>-P release rate was examined (Fig. 6). The Al+Fe-P release rate was obtained by examining the changes in the Al-P and Fe-P concentrations in the sediment, whereas the PO<sub>4</sub>-P release rate was determined from the change in the PO<sub>4</sub>-P concentration in the overlying water layer. Therefore, by comparing these two release rates, we tried to examine the correlation between the inorganic P concentration in the sediment and water layer. The Al+Fe-P release rate was positively correlated with the PO<sub>4</sub>-P release rate ( $p=0.0343$ ), suggesting that a large amount of P is released into the water layer when the Al+Fe-P release rate is high. As a result, the

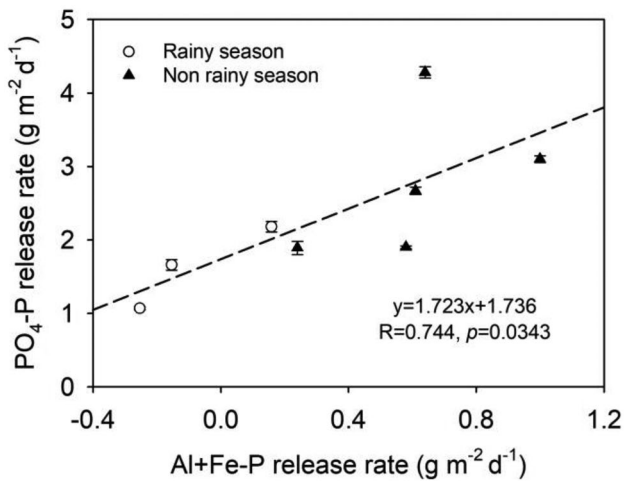


**Fig. 6** Correlation between the Al-P and Fe-P release rates and the  $\text{PO}_4\text{-P}$  release rate from the sediment to the water layer

properties of the sediments, which were different for each sampling period, significantly affected the P-fraction release rates. As evident from Fig. 6, the correlation between the Al+Fe-P release rate and the  $\text{PO}_4\text{-P}$  release rate can be classified by the sampling period—rainy and non-rainy seasons. Moreover, a higher  $\text{PO}_4\text{-P}$  release rate is expected from the sediments in the non-rainy season, resulting in a high P concentration in the overlying water layer.

The EF value of Al+Fe-P to Ca-P were ranged from 0.23 to 2.24 in day 0 sediment ( $n=36$ ), and were ranged from 0.12 to 4.10 in incubated sediment (3 and 7 days;  $n=36$ , respectively; Fig. 7). The EF value of the initial and incubated sediment was highest in Yeosu weir and lowest in Ipo weir, with greater variability in Yeosu weir than in Gangcheon and Ipo weir. According to previous studies, the ratio of Fe+Al-P and Ca-P is an effective indicator to

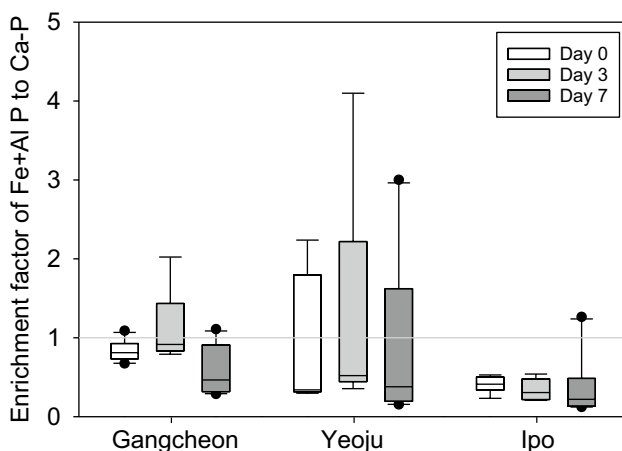


**Fig. 7** Changes in the enrichment factors (EF) of Fe+Al-P to Ca-P during the incubation (7 days) in the Gangcheon, Yeosu and Ipo weir

distinguish the relative contribution of point versus nonpoint sources among sediment samples in each weir (Zhang et al. 2022). In addition, the areas more affected by point sources showed dominant Fe/Al-bound P, while the areas more affected by nonpoint sources showed dominant Ca-bound P (Liu et al. 2012; Yang et al. 2020; Zhang et al. 2022). In the Gangcheon and Ipo weir, inorganic phosphorus derived from point source were 13% and 20%, respectively, and derived from nonpoint source were 87% and 80%, respectively. In Yeosu weir, inorganic phosphorus from point and nonpoint sources was 41% and 59%, respectively. Although nonpoint sources were dominant in the watershed of all weirs, there were more inorganic phosphorus derived from point source in Yeosu weir compared to other weirs. Most of the watershed of the Namhan River, where Gangcheon, Yeosu and Ipo weir are installed, consist of forest and agricultural areas (Lee et al. 2020). However, the point sources were high in the upstream of Yeosu weir, as there are many residential and commercial areas compared to other weirs. There is a Paldang Dam that supplies drinking water to the Seoul metropolitan area in the downstream of the Namhan River. The government of South Korea designated the Namhan River basin as a special water preservation area and has managed water quality by the total water pollution load management program and development restrictions. Therefore, as a result of the EF value, it is necessary to manage nonpoint source additionally to enhance the water quality downstream of the Gangcheon, Yeosu and Ipo weir. Especially, based on the results of EF value, more attention should be required on the Yeosu weir watershed to reduce the impact of point sources.

### 3.4 Relationship between the physiochemical factors and the P-fraction release rates

Linear regression analyses of the relationship between the physiochemical factors (overlying water pH,  $\text{NO}_x$ , and DOC; surface sediment TOC and chlorophyll-a contents; and  $\text{PO}_4\text{-P}$  release rate) and the P-fraction release rates were performed, and the corresponding results (Pearson's  $R$  values) are shown in Table 2 ( $n=12$ ). A positive Pearson's  $R$  value indicates a positive correlation, whereas a negative  $R$  value implies a negative correlation between the physiochemical factors and the P-fraction release rates. Evidently, the Al-P release rate is positively correlated with the pH ( $p=0.030$ ), consistent with the results of the previous studies, which demonstrated that a higher pH value corresponds to a weaker bonding between Al and P in the Al-P fraction (Nurnberg 1988; Orihel et al. 2017). Thus, Al-P content is easily released from the sediment to the water layer (Nurnberg 1988; Orihel et al. 2017). The organic matter ( $\text{NO}_x$  and DOC) in the overlying water showed correlation with the Fe-P, Ca-P, and Al+Fe+Ca-P release rates. The surface sediment TOC is correlated with the Fe-P

**Table 2** Pearson correlation between the physiochemical factors and the release rates of the various P fractions ( $n = 12$ )

Release rate	pH	Overlying water NO <sub>x</sub>	Overlying water DOC	Surface sediment TOC	Surface sediment chlorophyll-a
Al-P	0.713*	NS	NS	NS	NS
Fe-P	NS	-0.767*	-0.654*	0.716*	NS
Red-P	NS	NS	NS	NS	-0.658*
Ca-P	NS	-0.817**	-0.611*	NS	NS
Al+Fe-P	NS	NS	NS	NS	NS
Al+Fe+Ca-P	NS	-0.785*	NS	0.712*	NS

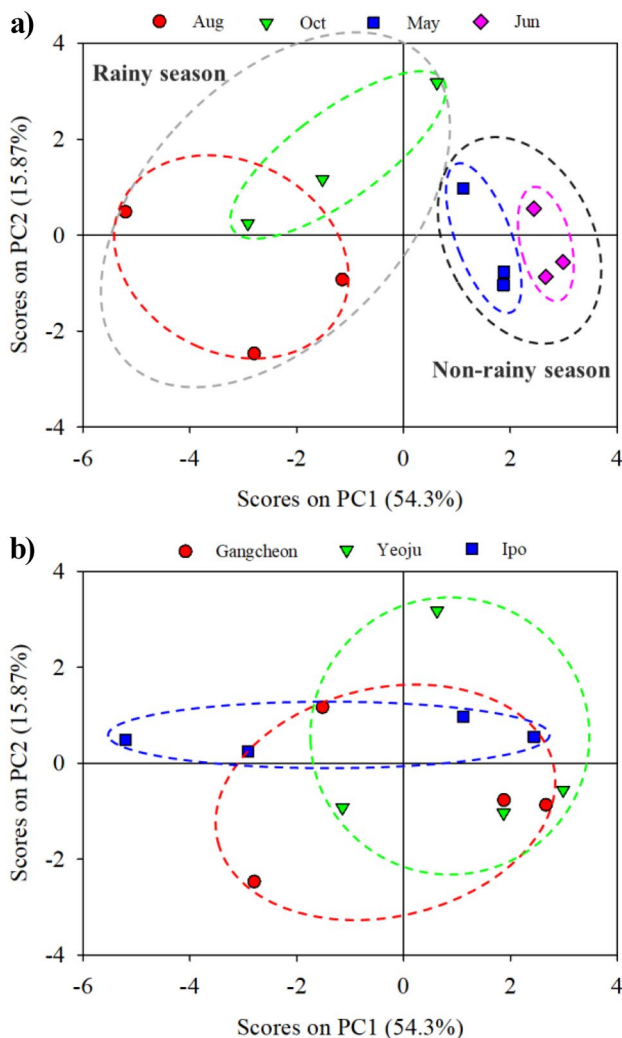
NS not significant

Significance level at  $p < 0.05$ \*;  $p < 0.01$ \*\*

( $p = 0.020$ ) and Al + Fe + Ca-P release rates ( $p = 0.020$ ). The metabolic activities of the microorganisms might be promoted by the organic matter, thereby influencing the P transformation in the sediment (Vincent et al. 2010; Shao

et al. 2019). Therefore, it is considered that the mineralization of the organic matter influenced the release of Fe-P and Al + Fe + Ca-P.

The PCA analysis was performed on the physiochemical factors with Pearson's  $R$  values of  $\pm 0.6$  or more, with no missing values ( $n = 12$ ). PC1 and PC2 were used according to the proportion of variance and cumulative proportion results. The first two PCs explain more than 70% of the data (PC1: 54.3% and PC2: 15.87%), and each point in the scatter plot represents one spectrum. PC1 describes the P fraction and precipitation, while PC2 describes the degree of decomposition of the organic matter. Figure 8a shows that PC1 and PC2 could lead to apparent clustering. The data obtained during the rainy season (August and October 2016) are located on the negative side of PC1, whereas those obtained during the non-rainy season (May and June 2017) tend to be distributed on the positive side of PC1. However, no obvious difference between the sampling locations is evident (Fig. 8b). Thus, the PCA results show that the P-fraction release rates and physiochemical factors changed with the sampling period rather than with the sampling location.

**Fig. 8** Score plots for PC1 and PC2 of the PCA result, as functions of sampling **a** time and **b** location

## 4 Conclusion

In this study, we investigated the temporal and spatial variations of the inorganic P fractions and their release using the sediment of three weirs built along the Han River in South Korea. Since three consecutive weirs of the Han River affect the P accumulation induced by rainfall which may affect the P release and cause long-term eutrophication of the impoundments; thus, this study was performed in an attempt to bridge this gap. There were significant temporal variations in the inorganic P fractions, the P release rate from the sediment, and the results of PCA analysis using physiochemical factors. The inorganic P fractions were significantly higher in the non-rainy season than in the rainy season. The Red-P and

Ca-P concentrations were high in the non-rainy season when there was less inflow of allochthonous organic matter. However, there were no significant spatial differences in the concentrations of Red-P and Ca-P. The incubation experimental results showed that the concentration of inorganic P in the sediments tended to decrease in the non-rainy season. The higher pH in the non-rainy season resulted in the more noticeable decrease of NAI-P, Al-P, and Fe-P, which could enhance the availability of P in the sediment. Inorganic P fractions could indicate relative contribution of point and non-point sources through the EF value. Sediments of three weirs were dominantly affected by nonpoint sources, but there was more inorganic phosphorus derived from point source in Yeosu weir which has residential and commercial areas in watershed. The positive correlation between the Al-P and Fe-P release rates and the PO<sub>4</sub>-P release rate suggested that the amount of P released into the water layer was large when the Al + Fe-P release rate was high. The correlation classified by the sampling period, i.e., rainy and non-rainy seasons, indicated a larger probability of a high PO<sub>4</sub>-P release rate from the sediment during the non-rainy season. The PCA results showed that the P-fraction release rate and physicochemical factors changed with the sampling period rather than with the sampling location. The results of this study showed that the sediment induced by rainfall affects the inorganic P fractions and the P release rate. To control the P release from the sediment and the water quality of the impounded water, it is necessary to establish water quality management strategies according to temporal variations. Measuring P releasing from sediment using the method of this study will help to implement water quality management in various water bodies with different hydrological characteristics and climates (Wang et al. 2005; Aydin et al. 2010; Thin et al. 2020). In addition, further studies are required to trace the sediment sources contributing to the variation of P pools within a river and to evaluate the dynamics of P in riverbed sediments. Extensive analysis of phosphorus content in sediments below as well as above the weir will be improve the understanding of change in bottom sediments properties due to the presence of hydro technical structure.

**Supplementary Information** The online version contains supplementary material available at <https://doi.org/10.1007/s11368-023-03459-1>.

**Author contribution** Jung Hyun Choi: conceptualization, methodology, writing-review and editing, supervision, funding acquisition; Haeseong Oh: validation, formal analysis, investigation, writing-original draft, project administration, writing-review and editing, visualization.

**Funding** This research was supported by the Basic Science Research Program through the National Research Foundation of Korea (NRF) funded by the Ministry of Education (2018R1A6A1A08025520 and 2016R1D1A1B04934910). Additional support was provided by the

Korea Ministry of Environment (Research on the effects of water quality due to environment of weir sediment) and the National Institute of Environmental Research in Korea.

**Data availability** The data used to support the findings of this study are available from the corresponding author upon request.

## Declarations

**Competing interests** The authors declare no competing interests.

## References

- Anzano J, Bonilla B, Montull-Ibor B, Casas-González J (2011) Plastic identification and comparison by multivariate techniques with laser-induced breakdown spectroscopy. *J Appl Polym Sci* 121:2710–2716. <https://doi.org/10.1002/app.33801>
- Aydin I, Aydin F, Hamamci C (2010) Phosphorus speciation in the surface sediment and river water from the Orontes (Asi) River. *Turkey Water Environ Res* 82(11):2265–2271. <https://doi.org/10.2175/106143010X12609736967206>
- Bao L, Li X, Su J (2020) Alteration in the potential of sediment phosphorus release along series of rubber dams in a typical urban landscape river. *Sci Rep* 10(1):1–10. <https://doi.org/10.1038/s41598-020-59493-3>
- Borggaard et al (1990) Influence of organic matter on phosphate adsorption by aluminium and iron oxides in sandy soils. *Eur J Soil Sci* 41:443–449. <https://doi.org/10.1111/j.1365-2389.1990.tb00078.x>
- Chen M, Kim SH, Jung HJ, Hyun JH, Choi JH, Lee HJ, Hur J (2017) Dynamics of dissolved organic matter in riverine sediments affected by weir impoundments: production, benthic flux, and environmental implications. *Water Res* 121:150–161. <https://doi.org/10.1016/j.watres.2017.05.022>
- Cho KJ, Jung HY, Shin JK (2002) Assessment of environment, nutrient dissolution and internal load contribution of low-grade sediments in the lower part of the Nakdong River. *Nakdong River* 62:2–13
- Furumai H, Kondo T, Ohgaki S (1989) Phosphorus exchange kinetics and exchangeable phosphorus forms in sediments. *Water Res* 23(6):685–691. [https://doi.org/10.1016/0043-1354\(89\)90200-5](https://doi.org/10.1016/0043-1354(89)90200-5)
- Hou D, He J, Lü C, Dong S, Wang J, Xie Z, Zhang F (2014) Spatial variations and distributions of phosphorus and nitrogen in bottom sediments from a typical north-temperate lake. *China Environ Earth Sci* 71(7):3063–3079. <https://doi.org/10.1007/s12665-013-2683-6>
- Huang H, Wang Z, Chen D, Xia F, Shang X, Liu Y, Mei K (2018) Influence of land use on the persistence effect of riverine phosphorus. *Hydrol Process* 32(1):118–125. <https://doi.org/10.1002/hyp.11408>
- Jalali M (2010) Phosphorus fractionation in river sediments, amadan, western Iran. *Soil Sediment Contam* 19(5):560–572. <https://doi.org/10.1080/15320383.2010.499927>
- Jensen HS, Andersen FO (1992) Importance of temperature, nitrate, and pH for phosphate release from aerobic sediments of four shallow, eutrophic lakes. *Limnol Oceanogr* 37(3):577–589. <https://doi.org/10.4319/lo.1992.37.3.0577>
- Jin G, Xu J, Mo Y, Tang H, Wei T, Wang YG, Li L (2020) Response of sediments and phosphorus to catchment characteristics and human activities under different rainfall patterns with Bayesian Networks. *J Hydrol* 584:124695. <https://doi.org/10.1016/j.jhydrol.2020.124695>
- Jun SH (1990) Forms and mobility of pollutants retained in the sediments from the Han River. *Kor J Lim* 23(1):31–42



- Kaiserli A, Voutsas D, Samara C (2002) Phosphorus fractionation in lake sediments—Lakes Volvi and Koronia. *N Greece Chemosphere* 46(8):1147–1155. [https://doi.org/10.1016/S0045-6535\(01\)00242-9](https://doi.org/10.1016/S0045-6535(01)00242-9)
- Kalbitz K, Schmerwitz J, Schwesig D, Matzner E (2003) Biodegradation of soil-derived dissolved organic matter as related to its properties. *Geoderma* 113(3–4):273–291. [https://doi.org/10.1016/S0016-7061\(02\)00365-8](https://doi.org/10.1016/S0016-7061(02)00365-8)
- Khare ND, Hesterberg D, Martin JD (2005) Xanes investigation of phosphate sorption in single and binary systems of iron and aluminum oxide minerals. *Environ Sci Technol* 39(7):2152–2160. <https://doi.org/10.1021/es049237b>
- Ki B, Lim B, Na EH, Choi JH (2010) A study on the nutrient release characteristics from sediments in the Asan Reservoir. *J Korean Soc Environ Eng* 32(1):1169–1176
- Kim G, Jeong W, Choi S (2005) Effects of water circulation on the phosphorus release rate from sediments in the lake. *J Korean Soc Water Environ* 21(6):595–601
- Kim LH, Choi E, Stenstrom MK (2003) Sediment characteristics, phosphorus types and phosphorus release rates between river and lake sediments. *Chemosphere* 50(1):53–61. [https://doi.org/10.1016/S0045-6535\(02\)00310-7](https://doi.org/10.1016/S0045-6535(02)00310-7)
- Kozerski HP, Kleeberg A (1998) The sediments and the benthic pelagic exchange in the shallow lake Muggelsee. *Int Rev Hydrobiol* 83:77–112. <https://doi.org/10.1002/iroh.19980830109>
- Lee JE, Choi JW, An GG (2012) Influence of landuse pattern and seasonal precipitation on the long-term physico-chemical water quality in Namhan River Watershed. *J Environ Sci* 21(9):1115–1129. <https://doi.org/10.5322/JES.2012.21.9.1115>
- Lee JW, Lee SW, An KJ, Hwang SJ, Kim NY (2020) An estimated structural equation model to assess the effects of land use on water quality and benthic macroinvertebrates in streams of the Namhan River System, South Korea. *Int J Environ Res Public Health* 17(6):2116. <https://doi.org/10.3390/ijerph17062116>
- Lee MH, Jung HJ, Kim SH, An SU, Choi JH, Lee HJ, Hur J (2018) Potential linkage between sediment oxygen demand and pore water chemistry in weir-impounded rivers. *Sci Total Environ* 619:1608–1617. <https://doi.org/10.1016/j.scitotenv.2017.10.141>
- Li H, Liu L, Li M, Zhang X (2013) Effects of pH, temperature, dissolved oxygen, and flow rate on phosphorus release processes at the sediment and water interface in storm sewer. *J Anal Methods Chem* 2013. <https://doi.org/10.1155/2013/104316>
- Liu E, Shen J, Birch GF, Yang X, Wu Y, Xue B (2012) Human-induced change in sedimentary trace metals and phosphorus in Chaohu Lake, China, over the past half-millennium. *J Paleolimn* 47(4):677–691. <https://doi.org/10.1007/s10933-012-9592-7>
- Luek JL, Thompson KE, Larsen RK, Heyes A, Gonsior M (2017) Sulfate reduction in sediments produces high levels of chromophoric dissolved organic matter. *Sci Rep* 7(1):8829. <https://doi.org/10.1038/s41598-017-09223-z>
- Ma SN, Wang HJ, Wang HZ, Li Y, Liu M, Liang XM, Søndergaard M (2018) High ammonium loading can increase alkaline phosphatase activity and promote sediment phosphorus release: a two-month mesocosm experiment. *Water Res* 145:388–397. <https://doi.org/10.1016/j.watres.2018.08.043>
- Némery J, Gratiot N, Doan PTK, Duvert C, Alvarado-Villanueva R, Duwig C (2016) Carbon, nitrogen, phosphorus, and sediment sources and retention in a small eutrophic tropical reservoir. *Aquat Sci* 78(1):171–189. <https://doi.org/10.1007/s00027-015-0416-5>
- Nürnberg GK (1988) Prediction of phosphorus release rates from total and reductant-soluble phosphorus in anoxic lake sediments. *Can J Fish Aquat Sci* 45(3):453–462. <https://doi.org/10.1139/f88-054>
- Oh H, Choi JH (2022) Changes in the dissolved organic matter characteristics released from sediment according to precipitation in the Namhan River with weirs: a laboratory experiment. *Int J Environ Res Public Health* 19(9):4958. <https://doi.org/10.3390/ijerph19094958>
- Oh HS, Huh IA, Choi JH (2017) Laboratory study of phosphorus fractionation in the sediments of Yeongsan River. *J Korean Soc Environ Eng* 39(9):519–526. <https://doi.org/10.4491/KSEE.2017.39.9.519>
- Olila OG, Redy KR (1997) Influence of redox potential on phosphorus uptake by sediments in two sub-tropical eutrophic lakes. *Hydrobiologia* 345:45–57. <https://doi.org/10.1023/A:1002975231341>
- Orihel DM, Baulch HM, Casson NJ, North RL, Parsons CT, Seckar DC, Venkiteswaran JJ (2017) Internal phosphorus loading in Canadian fresh waters: a critical review and data analysis. *Can J Fish Aquat Sci* 74(12):2005–2029. <https://doi.org/10.1139/cjfas-2016-0500>
- Park HK, Byeon MS, Choi MJ, Kim YJ (2008) The effect factors on the growth of phytoplankton and the sources of organic matters in downstream of Namhan River. *J Korean Soc Water Environ* 24(5):556–562
- Petersen GW, Corey RB (1966) A modified Chang and Jackson procedure for routine fractionation of inorganic soil phosphates. *Soil Sci Soc Am J* 30(5):563–565. <https://doi.org/10.2136/sssaj1966.03615995003000050012x>
- Renwick WH, Smith SV, Bartley JD, Buddemeier RW (2005) The role of impoundments in the sediment budget of the conterminous United States. *Geomorphology* 71(1–2):99–111. <https://doi.org/10.1016/j.geomorph.2004.01.010>
- Saha A, Jesna PK, Ramya VL, Mol SS, Panikkar P, Vijaykumar ME, Das BK (2022) Phosphorus fractions in the sediment of a tropical reservoir, India: implications for pollution source identification and eutrophication. *Environ Geochem Health* 44(3):749–769. <https://doi.org/10.1007/s10653-021-00985-0>
- Santos RMB, Fernandes LS, Pereira MG, Cortes RMV, Pacheco FAL (2015) A framework model for investigating the export of phosphorus to surface waters in forested watersheds: implications to management. *Sci Total Environ* 536:295–305. <https://doi.org/10.1016/j.scitotenv.2015.07.058>
- Shao W, Zhu J, Teng Z, Zhang K, Liu S, Li M (2019) Distribution of inorganic phosphorus and its response to the physicochemical characteristics of soil in Yeyahu Wetland, China. *Process Saf Environ Protect* 125:1–8. <https://doi.org/10.1016/j.psep.2019.02.025>
- Sun S, Huang S, Sun X, Wen W (2009) Phosphorus fractions and its release in the sediments of Haihe River. *China J Environ Sci* 21(3):291–295. [https://doi.org/10.1016/S1001-0742\(08\)62266-4](https://doi.org/10.1016/S1001-0742(08)62266-4)
- Thin MM, Sacchi E, Setti M, Re V (2020) A dual source of phosphorus to lake sediments indicated by distribution, content, and speciation: Inle Lake (Southern Shan State, Myanmar). *Water* 12(7):1993. <https://doi.org/10.3390/w12071993>
- Thurman EM (2012) Organic geochemistry of natural waters (Vol. 2). Springer Science & Business Media, Berlin
- Verma S, Subehia SK, Sharma SP (2005) Phosphorus fractions in an acid soil continuously fertilized with mineral and organic fertilizers. *Biol Fertil Soils* 41(4):295–300. <https://doi.org/10.1007/s00374-004-0810-y>
- Vilmin L, Aissa-Grouz N, Garnier J, Billen G, Mouchel JM, Poulin M, Flipo N (2015) Impact of hydro-sedimentary processes on the dynamics of soluble reactive phosphorus in the Seine River. *Biogeochemistry* 122(2):229–251. <https://doi.org/10.1007/s10533-014-0038-3>
- Vincent AG, Turner BL, Tanner EV (2010) Soil organic phosphorus dynamics following perturbation of litter cycling in a tropical moist forest. *Eur J Soil Sci* 61(1):48–57. <https://doi.org/10.1111/j.1365-2389.2009.01200.x>
- Vo NXQ, Ji Y, Doan TV, Kang H (2014) Distribution of inorganic phosphorus fractions in sediments of the South Han River over a rainy season. *Environ Eng Res* 19(3):229–240. <https://doi.org/10.4491/eer.2014.026>
- Wang S, Jin X, Pang Y, Zhao H, Zhou X, Wu F (2005) Phosphorus fractions and phosphate sorption characteristics in relation to the sediment compositions of shallow lakes in the middle and lower



- reaches of Yangtze River region. *China J Colloid Interface Sci* 289(2):339–346. <https://doi.org/10.1016/j.jcis.2005.03.081>
- Wu B, Wan J, Zhang Y, Pan B, Lo IMC (2020) Selective phosphate removal from water and wastewater using sorption: process fundamentals and removal mechanisms. *Environ Sci Technol* 54:50–66. <https://doi.org/10.1021/acs.est.9b05569>
- Wu Y, Wen Y, Zhou J, Wu Y (2014) Phosphorus release from lake sediments: effects of pH, temperature and dissolved oxygen. *Ksce J Civ Eng* 18(1):323–329. <https://doi.org/10.1007/s12205-014-0192-0>
- Yang P, Yang C, Yin H (2020) Dynamics of phosphorus composition in suspended particulate matter from a turbid eutrophic shallow lake (Lake Chaohu, China): implications for phosphorus cycling and management. *Sci Total Environ* 741:140203. <https://doi.org/10.1016/j.scitotenv.2020.140203>
- Yao Y, Wang P, Wang C, Hou J, Miao L, Yuan Y, Liu C (2016) Assessment of mobilization of labile phosphorus and iron across sediment-water interface in a shallow lake (Hongze) based on in situ high-resolution measurement. *Environ Pollut* 219:873–882. <https://doi.org/10.1016/j.envpol.2016.08.054>
- Zhang J, Buyang S, Yi Q, Deng P, Huang W, Chen C, Shi W (2022) Connecting sources, fractions and algal availability of sediment phosphorus in shallow lakes: an approach to the criteria for sediment phosphorus concentrations. *J Environ Sci* 125:798–810. <https://doi.org/10.1016/j.jes.2022.03.038>
- Zhou Q, Gibson CE, Zhu Y (2001) Evaluation of phosphorus bio-availability in sediments of three contrasting lakes in China and the UK. *Chemosphere* 42(2):221–225. [https://doi.org/10.1016/S0045-6535\(00\)00129-6](https://doi.org/10.1016/S0045-6535(00)00129-6)

**Publisher's Note** Springer Nature remains neutral with regard to jurisdictional claims in published maps and institutional affiliations.

Springer Nature or its licensor (e.g. a society or other partner) holds exclusive rights to this article under a publishing agreement with the author(s) or other rightsholder(s); author self-archiving of the accepted manuscript version of this article is solely governed by the terms of such publishing agreement and applicable law.